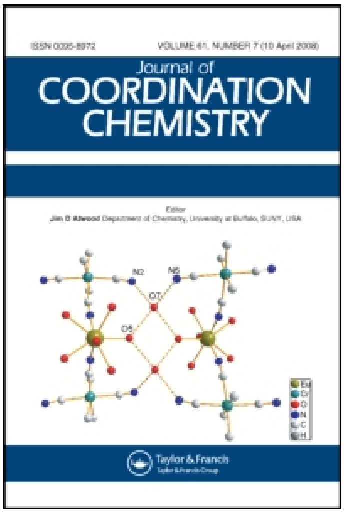

Journal of Coordination Chemistry
Publication details, including instructions for authors and subscription information:
http://www.informaworld.com/smpp/title~content=t713455674

Synthesis and crystal structures of two new zigzag *versus* helical coordination polymers based on diphenic acid

Feng Guo[a]; Baoyong Zhu[a]; Xiuling Zhang[a]; Yulan Song[a]; Ping Wu[a]
[a] Department of Chemistry, Dezhou University, Shandong 253023, P.R. China

To cite this Article Guo, Feng , Zhu, Baoyong , Zhang, Xiuling , Song, Yulan and Wu, Ping(2010) 'Synthesis and crystal structures of two new zigzag *versus* helical coordination polymers based on diphenic acid', Journal of Coordination Chemistry, 63: 7, 1130 — 1138, First published on: 26 March 2010 (iFirst)

To link to this Article: DOI: 10.1080/00958971003735465

URL: http://dx.doi.org/10.1080/00958971003735465

Journal of Coordination Chemistry
Vol. 63, No. 7, 10 April 2010, 1130–1138

Synthesis and crystal structures of two new zigzag *versus* helical coordination polymers based on diphenic acid

FENG GUO*, BAOYONG ZHU, XIULING ZHANG,
YULAN SONG and PING WU

Department of Chemistry, Dezhou University,
Shandong 253023, P.R. China

(*Received 17 September 2009; in final form 2 December 2009*)

Two new coordination polymers, $[Mn(dpa)(2,2'\text{-bipy})]_n$ (**1**) and $[Ni(dpa)(2,2'\text{-bipy})]_n$ (**2**) ($H_2dpa = 3,4'$-biphenyl-dicarboxylic acid, 2,2′-bipy = bipyridine), have been synthesized and structurally characterized by elemental analysis, IR, and X-ray diffraction. Single-crystal X-ray analyses revealed that 3,4′-diphenic acid acts as a bridging ligand, exhibiting rich coordination modes to link metal ions: μ_2–η^1: η^1, μ_1–η^1: η^1, and μ_1–η^1: η^0. Compound **1** demonstrates a 1-D zigzag chain. Compound **2** is a 1-D helical chain. In **1** and **2**, there exist intermolecular π–π stacking interactions and non-covalent interactions responsible for the stabilization of the supramolecular structure. In **1**, the Mn(II) chains exhibit a weak antiferromagnetic interaction.

Keywords: Coordination polymer; Hydrothermal synthesis; Crystal structure

1. Introduction

Owing to the intriguing structural features and potential applications in gas storage, the catalysis, separations, nonlinear optics, molecular magnetism, and luminescence, coordination polymers have attracted considerable interest [1–4]. Rational design and synthesis of coordination polymers have received unprecedented attention from chemists and material scientists [5]. Carboxylates have been used as bridges in coordination chemistry for a long time and are excellent candidates to design and construct various molecular structures with beautiful aesthetics and useful functional properties [6–9]. N-containing ligands have been employed in the preparation of coordination polymers, providing potential supramolecular recognition sites for π–π aromatic stacking interactions [10].

Diphenic acid (H_2dpa) as an O-donor has received attention in the designed synthesis of coordination polymers [11, 12]. In this article, we select 3,4′-dpa for the following reasons. First, the two functional groups may have different coordination modes in H_2dpa with an ability to generate metal–oxygen chains or clusters [13–15]. Second, in

---

*Corresponding author. Email: guofeng1510@yeah.net

Journal of Coordination Chemistry
ISSN 0095-8972 print/ISSN 1029-0389 online © 2010 Taylor & Francis
DOI: 10.1080/00958971003735465

deprotonated H_2dpa, two phenyl rings are not coplanar owing to the steric hindrance of carboxylates in coordination. The distortion of diphenyl spacer about the central bond allows dpa to link metal ions or metal clusters into helical chains or 1-D chains [16, 17]. In this article, we have synthesized two new coordination polymers, $[\mathrm{Mn(dpa)(2,2'\text{-}bipy)}]_n$ (**1**) and $[\mathrm{Ni(dpa)(2,2'\text{-}bipy)}]_n$ (**2**), based on 3,4′-dpa.

2. Experimental

2.1. *General materials and method*

All reagents and solvents were commercially available and used as received. Elemental analysis was carried out on a Carlo Erba 1106 full-automatic trace organic elemental analyzer. FT-IR spectra were recorded with a Bruker Equinox 55 FT-IR spectrometer as dry KBr pellets from 400 to 4000 $\mathrm{cm^{-1}}$.

2.2. *Preparation of compounds*

2.2.1. $[\mathrm{Mn(dpa)(2,2'\text{-}bipy)}]_n$ (1). The hydrothermal reaction of $MnCl_2 \cdot 4H_2O$ (0.099 g, 0.5 mmol), H_2dpa (0.121 g, 0.5 mmol), 2,2′-bipy (0.156 g, 1 mmol), NaOH (0.04 g, 1 mmol), and distilled water (18 mL) was heated to 160°C for 96 h in a 25 mL stainless steel reactor with a Teflon liner, followed by slow cooling to room temperature. The resulting yellow block crystals were washed with alcohol to give pure samples (Yield: 62% based on Mn). Elemental Anal. Calcd (%) for $C_{24}H_{16}MnN_2O_4$: C, 63.87; H, 3.57; N, 6.21. Found (%): C, 64.18; H, 3.73; N, 6.14. IR: 1618 s, 1584 s, 1567 s, 1435 s, 1302 w, 1195 w, 860 m, 616 m.

2.2.2. $[\mathrm{Ni(dpa)(2,2'\text{-}bipy)(H_2O)}]_n$ (2). The hydrothermal reaction of $NiCl_2 \cdot 6H_2O$ (0.119 g, 0.5 mmol), H_2dpa (0.121 g, 0.5 mmol), NaOH (0.04 g, 1 mol), 2,2′-bipy (0.156 g, 1 mmol), and distilled water (18 mL) was heated to 140°C for 72 h in a 25 mL stainless steel reactor with a Teflon liner, followed by slow cooling to room temperature. The resulting green block crystals were washed with alcohol to give pure samples (Yield: 60% based on Ni). Elemental Anal. Calcd (%) for $C_{24}H_{18}N_2NiO_5$: C, 60.93; H, 3.83; N, 5.92. Found (%): C, 60.86; H, 3.84; N, 6.07. IR: 3396 br, 3017 w, 1627 s, 1582 s, 1527 w, 1463 m, 1426 m, 1238 w, 1087 w, 1061 m, 1021 w, 830 m, 802 s, 717 w, 644 w, 561 m.

2.3. *X-ray crystallography*

Suitable single crystals of **1** and **2** were selected under a polarizing microscope and fixed with an epoxy on fine glass fibers and mounted on a Bruker Smart 1000 CCD diffractometer with Mo-Kα radiation ($\lambda = 0.71073$ Å) at 293(2) K by using an ω-scan mode for cell determination and data collection. All non-hydrogen atoms were located by direct methods and subsequent difference Fourier syntheses. The hydrogens bound to carbon were located by calculation and their positions and thermal parameters were fixed during refinement. All non-hydrogen atoms were refined by full-matrix least-squares techniques and all calculations were performed by SHELXTL 97 [18]. Crystal data, intensity collection, and structure refinement details are summarized in table 1. Selected interatomic distances and angles are given in table 2.

3. Results and discussion

3.1. *Structure description*

3.1.1. [Mn(dpa)(2,2′-bipy)]$_n$ (1). Crystallographic analysis reveals that [Mn(dpa)(2,2′-bipy)]$_n$ crystallizes in the monoclinic system, space group *C2/c*. The coordination environment around Mn(II) (figure 1) consists of dinuclear units of Mn(II), where each pair of Mn(II)'s is linked by two dpa anions with an Mn $\cdots$ Mn separation of 4.823 Å. The Mn(1) exhibits octahedral geometry, with an N_2O_4 coordination sphere from three dpa ligands [Mn(1)–O(1) = 2.292(1) Å, Mn(1)–O(2) = 2.233(1) Å, Mn(1)–O(3) = 2.103(1) Å and Mn(1)–O(4) = 2.103(1) Å], and one 2,2′-bipy [Mn(1)–N(1) = 2.242(19) Å and Mn(1)–N(2) = 2.263(2) Å]. Dpa is a μ_3-ligand (μ_2–η^1: η^1 and μ_1–η^1: η^1, shown in scheme 1a) with one carboxylate bridging two Mn(II)'s bis-monodentate, and the other carboxylate bridging another Mn(II) through a bidentate chelating mode. The organic ligands link Mn(II) nodes to form a 1-D zigzag chain (figure 2). Dihedral angle between two phenyl rings in dpa ligands is 34.09°. The 2,2′-bipy ligands are alternately attached to both sides of the zigzag chain, providing potential supramolecular recognition sites for π–π stacking interactions. The interchain distance between parallel 2,2′-bipy's is *ca* 3.64 Å and the corresponding centroid-to-centroid

Table 1. Crystallographic data and structure refinement summary for **1** and **2**.

Empirical formula	$C_{24}H_{16}MnN_2O_4$	$C_{24}H_{18}N_2NiO_5$
Formula weight	451.33	473.11
Crystal system	Monoclinic	Monoclinic
Space group	*C2/c*	*P2₁/c*
Unit cell dimensions (Å, °)		
a	13.542(5)	6.832(5)
b	15.256(5)	17.940(5)
c	20.071(5)	16.764(5)
α	90.000	90.000
β	91.496(5)	97.344(5)
γ	90.000	90.000
Volume (Å^3), *Z*	4145(2), 8	2037.8(17), 4
Calculated density (mg m^{-3})	1.446	1.542
F(000)	1848	976
θ range for data collection (°)	2.24–27.99	2.58–28.18
Limiting indices	$-17 \le h \le 15$; $-20 \le k \le 17$; $-26 \le l \le 15$	$-8 \le h \le 7$; $-15 \le k \le 23$; $-21 \le l \le 22$
Goodness-of-fit on F^2	1.042	1.127
Final *R* indices [$I > 2\sigma(I)$]	$R_1 = 0.330$; $wR_2 = 0.0776$	$R_1 = 0.0385$; $wR_2 = 0.1270$
R indices (all data)	$R_1 = 0.0470$; $wR_2 = 0.0842$	$R_1 = 0.0459$; $wR_2 = 0.1407$
Largest difference peak and hole (e Å^{-3})	0.249 and −0.244	0.537 and −0.739

$wR_2 = [\sum w(F_o^2 - F_c^2)^2/\sum w(F_o^2)^2]^{1/2}$; $w = 1/[\sigma^2(F_o)^2 + (AP)^2 + BP]$ with $P = (F_o^2 + 2F_c^2)/3$.

Table 2. Selected bond lengths (Å) and angles (°) for **1** and **2**.

1			
Mn(1)–O(1)#1	2.292(1)	Mn(1)–O(3)	2.103(1)
Mn(1)–O(2)#1	2.233(1)	Mn(1)–O(4)	2.103(1)
Mn(1)–N(1)	2.271(2)	Mn(1)–N(2)	2.263(2)
O(4)–Mn(1)–O(3A)#2	94.08(6)	O(4)–Mn(1)–O(2)#1	91.97(5)
O(3)–Mn(1)–O(2)#1	104.61(6)	O(4)–Mn(1)–N(2)	110.31(5)
O(3A)#2–Mn(1)–N(2)	91.90(5)	O(2)#1–Mn(1)–N(2)	151.36(5)
O(4)–Mn(1)–N(1)	92.87(6)	O(3A)#2–Mn(1)–N(1)	163.73(5)
O(2)#1–Mn(1)–N(1)	89.82(5)	N(2)–Mn(1)–N(1)	71.88(5)
O(4)–Mn(1)–O(1)#1	149.95(5)	O(3A)#2–Mn(1)–O(1)#1	91.21(6)
O(2)#1–Mn(1)–O(1)#1	58.12(4)	N(2)–Mn(1)–O(1)#1	99.03(5)
2			
Ni(1)–O(1)#1	2.057(2)	Ni(1)–O(2)#1	2.280(2)
Ni(1)–N(1)	2.059(2)	Ni(1)–N(2)	2.064(2)
Ni(1)–O(4)	1.995(2)	Ni(1)–O(1w)	2.085(2)
O(4)–Ni(1)–O(1)#1	90.46(8)	O(4)–Ni(1)–N(1)	92.60(9)
O(1)#1–Ni(1)–N(1)	168.59(8)	O(4)–Ni(1)–N(2)	169.26(8)
O(1)#1–Ni(1)–N(2)	96.58(8)	N(1)–Ni(1)–N(2)	78.96(8)
O(4)–Ni(1)–O(1w)	92.38(8)	O(1)#1–Ni(1)–O(1w)	98.59(8)
N(1)–Ni(1)–O(1w)	92.26(8)	N(2)–Ni(1)–O(1w)	94.57(8)
O(4)–Ni(1)–O(2)#1	86.30(8)	O(1)#1–Ni(1)–O(2)#1	60.79(7)
N(1)–Ni(1)–O(2)#1	108.44(8)	N(2)–Ni(1)–O(2)#1	90.06(8)

Symmetry code for compounds: (**1**) #1: $-x$, $1-y$, $-z$; #2: $2-x$, y, $0.5-z$; (**2**) #1: $-x$, $-0.5+y$, $0.5-z$.

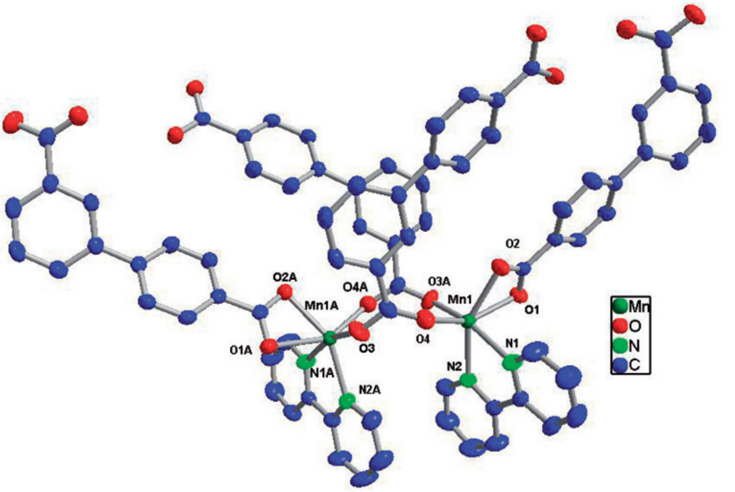

Figure 1. View of **1** showing the coordination environment of Mn(II). All hydrogen atoms are omitted for clarity.

distance is *ca* 3.896 Å, indicating face-to-face π–π stacking interactions that further stabilize the crystal structure (figure 3).

3.1.2. $[Ni(dpa)(2,2'\text{-}bipy)(H_2O)]_n$ (2). The local coordination geometry of $[Ni(dpa)(2,2'\text{-}bipy)(H_2O)]_n$ with atom-numbering scheme is shown in figure 4, with

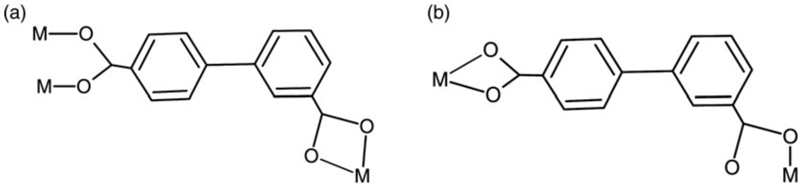

Scheme 1. The coordination modes of dpa: (a) μ_2–η^1: η^1/μ_1–η^1: η^1 and (b) μ_1–η^1: η^1/μ_1–η^1: η^0.

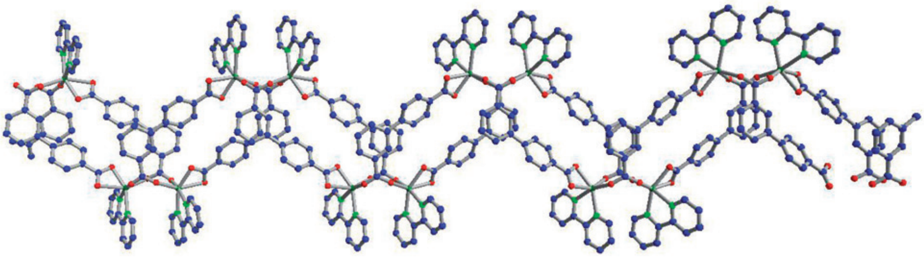

Figure 2. The 1-D zigzag chain running along the *c*-axis in **1**.

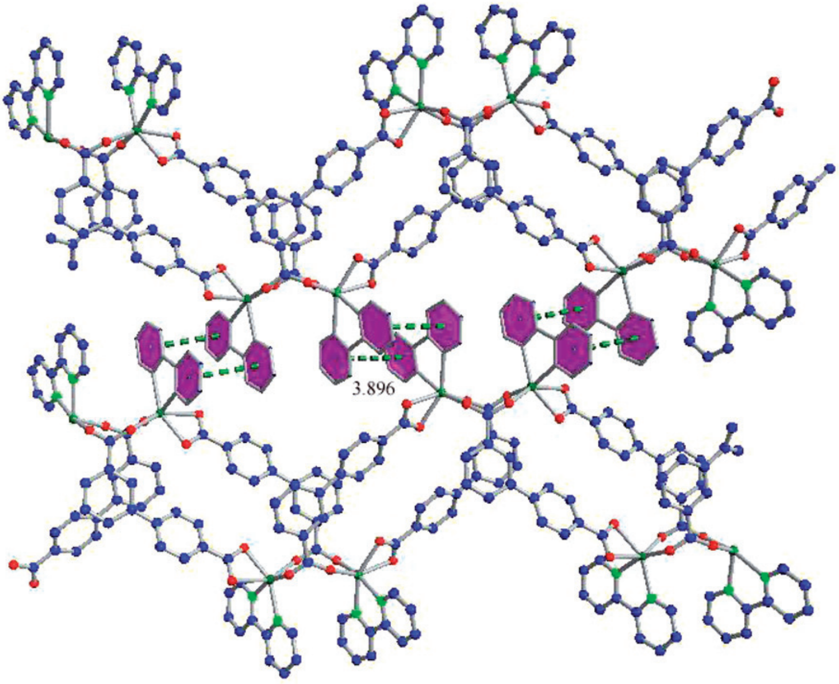

Figure 3. The 2-D supramolecular structure through π–π interactions for **1**.

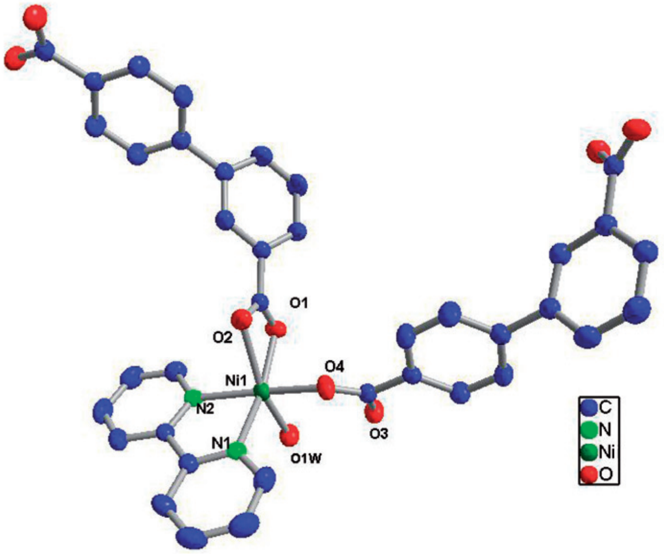

Figure 4. Coordination environment of Ni(II) in **2** with 50% probability thermal ellipsoids. All hydrogen atoms are omitted for clarity.

Ni(II) coordinated by three oxygens from two dpa ligands, one coordinated water [Ni(1)–O(1) = 2.057(2) Å, Ni(1)–O(2) = 2.280(2) Å, Ni(1)–O(4) = 1.995(2) Å, and Ni(1)–O(1w) = 2.085(2) Å], and two nitrogens from 2,2′-bipy ligands [Ni(1)–N(1) =2.059(2) Å and Ni(1)–N(1) = 2.059(2) Å] in a distorted octahedral geometry. The dihedral angle between two phenyl rings is 62.96° and the dihedral angles of carboxylates and the corresponding linking ring is 33.26° and 24.30°, respectively. The 3,4′-dpa is a μ_2-bridge, linking two Ni(II)'s through a bidentate chelating carboxylate and a monodentate carboxylate (μ_1–η^1: η^1/μ_1–η^1: η^0, shown in scheme 1b) forming a 1-D helical chain along the *c*-axis, with a pitch of 17.940 Å (figure 5). Two adjacent helical chains with different handedness are assembled by intermolecular π–π stacking which is similar to the structures of [Cd_2Cl_2(1,3-BDC)$(TTBT)_2(H_2O)$] and [CdCl(1,4-HBDC)(TTBT)] [19]. The interplanar distance between neighboring parallel 2,2′-bipy groups is *ca* 3.45 Å, and the corresponding centroid-to-centroid distance is *ca* 3.59 Å (figure 6).

3.2. *Magnetic measurements*

Variable temperature magnetic susceptibility measurements of powdered sample of **1** from 2 to 300 K gave χT of 8.72 emu K mol^{-1}, close to the spin-only value of 8.75 emu K mol^{-1} with $g = 2.00$ for two adjacent Mn(II) ions. When temperature is lowered, χT decreases gradually until ~50 K and then sharply decreases to 0.84 emu K mol^{-1} (figure 7), characteristic of antiferromagnetic coupling. The data were fitted to the conversional equation derived by Fisher for infinite chain model based on the Hamiltonian $\hat{H} = -2\sum J\hat{\mathrm{S}}_{\mathrm{i}}\hat{\mathrm{S}}_{\mathrm{i+1}}$ [20]:

$$\chi_{\mathrm{M}}^{\mathrm{chain}} = Ng^2\beta^2\{S_{\mathrm{Mn}}(S_{\mathrm{Mn}}+1)/3KT\}\{(1+\mu)/(1-\mu)\} \tag{1}$$

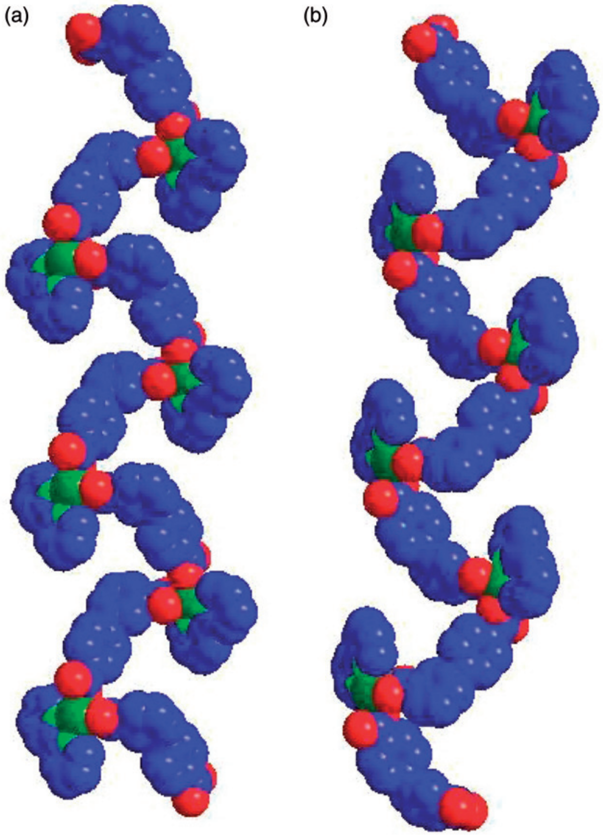

Figure 5. Space-filling model to (a) left-handed and (b) right-handed helical chains.

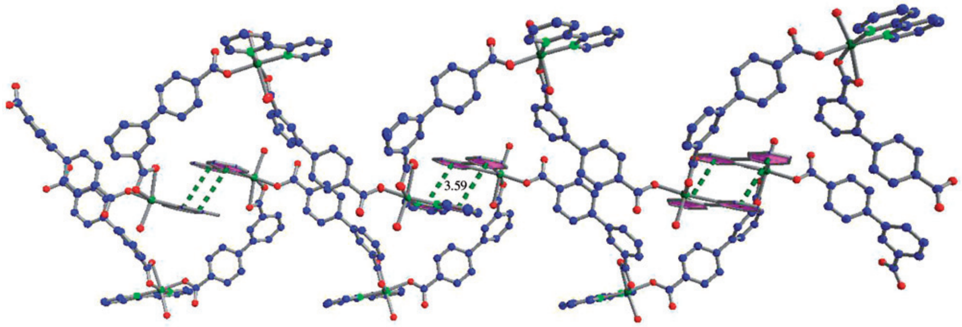

Figure 6. The 2-D supramolecular structure through π–π interactions.

where μ is the Langevin function defined as $\mu = \coth[JS_{\mathrm{Mn}}(S_{\mathrm{Mn}}+1)/KT]-[KT/JS_{\mathrm{Mn}}(S_{\mathrm{Mn}}+1)]$ with $S = 5/2$ and J refers to the interaction between adjacent Mn(II) ions. The J value [$-2.32(1)$ cm^{-1}] also suggests weak antiferromagnetic interactions between the neighboring Mn(II) ions mediated through carboxylate bridges.

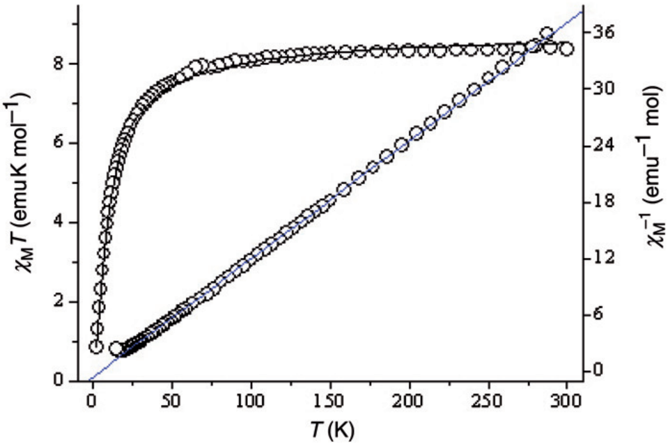

Figure 7. Thermal variation of χT and χ^{-1} of **1**. The solid lines represent the best fit to the equation.

The J value is comparable to those reported for other manganese(II) complexes with bridging carboxylate, which generally mediate weak magnetic interactions [20–22].

4. Conclusions

The assembly of Mn and Ni with dpa in the presence of 2,2′-bipy gives two frameworks with distinct structural features. When changing from Mn(II) to Ni(II), the structure changes from 1-D zigzag chain to 1-D helical structure. Additional π–π stacking interactions extend and stabilize the coordination motifs. The magnetic coupling in **1** was found to be antiferromagnetic with $J_{\mathrm{Mn}} = -2.32(1)\ \mathrm{cm}^{-1}$.

Supplementary material

Crystallographic information of the three compounds has been deposited with the Cambridge Crystallographic Data Centre as supplementary publication number CCDC 748090 for $[\mathrm{Mn(dpa)(2,2'\text{-}bipy)}]_n$ and CCDC 748091 for $[\mathrm{Ni(dpa)(2,2'\text{-}bipy)}]_n$. Copies of the data may be obtained free of charge on application to CCDC, 12 Union Road, Cambridge CB2 1EZ, UK (Fax: +44-1223-336-033; Email: deposit@ccdc.cam.ac.uk or www: http://www.ccdc.cam.ac.uk).

Acknowledgments

The authors gratefully acknowledge the financial support from the National Natural Science Foundation of China (20971018).

References

[1] M. Eddaoudi, D.B. Moler, H.L. Li, B.L. Chen, T.M. Reineke, M. O'Keeffe, O.M. Yaghi. *Acc. Chem. Res.*, **34**, 319 (2001).

[2] D. Maspoch, D. Ruiz-Molina, J. Veciana. *J. Mater. Chem.*, **14**, 2713 (2004).

[3] J.F. Eubank, V.C. Kravtsov, M. Eddaoudi. *J. Am. Chem. Soc.*, **129**, 5820 (2007).

[4] Q. Ye, X.S. Wang, H. Zhao, R.G. Xiong. *Chem. Soc. Rev.*, **34**, 208 (2005).

[5] L. Murray, M. Dinca, J.R. Long. *Chem. Soc. Rev.*, **38**, 1294 (2009).

[6] M. Eddaoudi, J. Kim, N. Rosi, D. Vodak, J. Wachter, M. O'Keeffe, O.M. Yaghi. *Science*, **295**, 469 (2002).

[7] R.Q. Fang, X.H. Zhang, X.M. Zhang. *Cryst. Growth Des.*, **6**, 2637 (2006).

[8] S.M. Humphrey, R.A. Mole, M. McPartlin, E.J.L. McInnes, P.T. Wood. *Inorg. Chem.*, **46**, 5981 (2005).

[9] X.N. Cheng, W.X. Zhang, Y.Z. Zheng, X.M. Chen. *Chem. Commun.*, 3603 (2006).

[10] F. Nouar, J.F. Eubank, T. Bousquet, L. Wojtas, M.J. Zaworotko, M. Eddaoudi. *J. Am. Chem. Soc.*, **130**, 1833 (2008).

[11] R.H. Wang, Y.F. Zhou, Y.Q. Sun, D.Q. Yuan, L. Han, B.Y. Lou, B.L. Wu, M.C. Hong. *Cryst. Growth Des.*, **5**, 251 (2005).

[12] R.H. Wang, Y.Q. Gong, L. Han, D.Q. Yuan, B.Y. Lou, B.L. Wu, M.C. Hong. *J. Mol. Struct.*, **784**, 1 (2006).

[13] Y. Wang, X. Zheng, W. Zhuang, L. Jin. *Eur. J. Inorg. Chem.*, 1355 (2003).

[14] R.H. Wang, D.Q. Yuan, F.L. Jiang, L. Han, Y.Q. Gong, M.C. Hong. *Cryst. Growth Des.*, **6**, 1351 (2006).

[15] X.L. Wang, C. Qin, E.B. Wang, Z.M. Su. *Chem. Eur. J.*, **12**, 1280 (2006).

[16] Z. Shi, L. Zhang, S. Gao, G.Y. Yang, J. Hua, L. Gao, S.H. Feng. *Inorg. Chem.*, **39**, 1990 (2000).

[17] K.J. Arm, W. Leslie, J.A.G. Williams. *Inorg. Chim. Acta*, **359**, 1222 (2006).

[18] G.M. Sheldrick. *SHELXS-97 and SHELXL-97, Program for X-ray Crystal Structure Solution and Refinement*, Göttingen University, Göttingen, Germany (1997).

[19] G.B. Che, J. Wang, B. Liu, X.Y. Li, C.B. Liu. *J. Coord. Chem.*, **62**, 302 (2009).

[20] M.E. Fisher. *Am. J. Phys.*, **32**, 343 (1964).

[21] Q.X. Jia, W.W. Sun, C.F. Yao, H.H. Wu, E.Q. Gao, C.M. Liu. *Dalton Trans.*, 2721 (2009).

[22] L. Han, Y. Zhou, X.T. Wang, X. Li, M.L. Tong. *J. Mol. Struct.*, **923**, 24 (2009).